ISSN No. 2454-6194 | DOI: 10.51584/IJRIAS | Volume VIII Issue VI June 2023

Frequency-Domain Electromagnetic and VLF Data with An Application to Modeling of Basement Structures: A Case Study Within, Ibadan Area, Southwestern Nigeria

***Abdulbariu Ibrahim[1], Baba Aminu Mu'awiya[1], Achonwa Kingsley Okechukwu[2]**

[1]Department of Geology, Federal University Lokoja, Kogi State, Nigeria.
[2]Department of Chemical/Petrochemical Engineering, Rivers State University, Port Harcourt

DOI: https://doi.org/10.51584/IJRIAS.2023.8616

Received: 11 May 2023; Revised: 08 June 2023; Accepted: 13 June 2023; Published: 13 July 2023

Abstract: The study area, the church camp is within Ibadan which fall within southwestern basement complex of Nigeria and it is mainly by migmatite-gneiss. The hard rocks are usually characterized by basement fracture which may serve as a conduit for groundwater passage. This has necessitated detail geological and geophysical investigation to accurately and precisely delineate this structure. Geological mapping alongside very low frequency Electromagnetic (VLF-EM) techniques were adopted in which conductivity data were acquired along Fifteen (15) VLF profiles using ABEM WADI. Thirteen (13) of these profiles were in the East-West (E-W) direction which is the dip direction of the structural elements, while the remaining two profiles were in North-South (N-S) direction. The data obtained from the field were processed, filtered and presented inform of profiles and Karous-Hjelt (K-H) filtered pseudo-section to visualise conductivity in (2-D). Pockets of conductive structures were delineated and were interpreted as fractures of various dimension and orientation. Some are single fracture and others are closely-spaced double fractures which some of them joined or fused together at depth with some suspected to contain water while some are dry base on their conductivity/resistivity signature exhibited. In conclusion, VLF-EM has proven to possess the capability to characterize and model the basement fractures and define their dimension, axial orientation and indicates their parallelism which also signifies their origin as regard stress regime that produces the fracture.

Keywords: Migmatite-gneiss, VLF-EM, fracture, Karous-Hjelt pseudo-section, Conductivity.

I. Introduction

The basement complex of Nigeria covers almost fifty percent of the entire land mass of the country. They are hard rocks characterized by low porosity and relatively impermeable but in some cases they fractured due to tectonic episode. It is in this fractures that groundwater occurs. A typical Basement Complex terrain distinguished by the presence of hills and mountains thereby making access to potable water is challenging. Changde et al (2022) and Andarawus et al (2022) asserted that due to the complexities associated with Basement Complex terrains, proper understanding of the hydrogeological characteristics of the auriferous units is imperative for sustainable exploitation and development of groundwater resources. Groundwater exploitation in basement-complicated terrain necessitates a thorough grasp of its hydrological properties. Groundwater is mostly trapped in permeable and leaky weathered areas in the Basement Complex terrain.

Therefore, the need to effectively characterize this network of basement feature can never be over emphasize because of their importance. In this regard, geophysical method was adopted at 'GOFAMINT Church Camp, Ibadan, Southwestern Nigeria where Very Low Frequency Electromagnetic (VLF-EM) was used to delineate the basement structure.

The VLF-EM serve for the quick identification of high conductivity anomalous zone thought to be due to conducting Orebody, intense weathering and| or fracture zones. Its great advantage is in its ability to identify steeply to vertically dipping fracture surface with conductive minerals and or water.

Previous Work

According to Iseshien-Emekeme et al. (2004), Ezeh and Ugwu (2010), Anomohanran (2011a, b), Atakpo, Muawiya et al. (2022), and Ofomola (2012), electromagnetic and electrical resistivity techniques are the most frequently and widely used in geophysical techniques for groundwater exploration and basement studies. Faruk (2019) inferred that this is because their field instrument operations are simpler, more user-friendly, and their data analysis is cost-effective,

The VLF-EM method is effective for accelerated geological mapping and searching for buried conductive targets. It is a reliable technique for identifying network of fractures usually hidden by overburden materials that overlie the crystalline basement . The method utilizes signal radiation from military navigation radio transmitters. There are about 42 global ground military communication transmitters (ABEM 2007) operating in the VLF range of 15–30 kHz. These stations, sighted around the globe,

ISSN No. 2454-6194 | DOI: 10.51584/IJRIAS | Volume VIII Issue VI June 2023

generate effective signals used for a diverse range of applications which includes navigation and communication, groundwater detection or contamination, soil engineering, ionospherical, meteorological, archeological and VLF band transmission studies, other applications include: mineral exploration, mapping of fault zones, etc. (Wright 1988, Ramesh-Babu et al 2007, Sundararajan et al 2007).

Also, (VLF-EM) prospecting method is suitable for studying structural details and shallow subsurface conductors according to Fisher et al., 1983 because it is not only rapid but also effective in terms of cost.

Magawata et al. (2019) further involved (VLF-EM) application in which can be characterized as the detection of electromagnetic anomalies caused by induction from a primary magnetic field. For this reason, the VLF method has proven to be an effective exploration tool for massive sulphides, graphite, carbonaceous shales, sheared contacts and fracture zones. Therefore, over the last few decades, it has been employed globally to identify conductive features in mineral exploration, geological, engineering and environmental problems (Phillips and Richards 1975, Parker, 1980, Saydam 1981, Hayles and Sinha 1986, Ogilvy and Lee 1991, Ramesh Babu et al 2007, Sundararajan et al 2007).

Although the VLF-EM has been widely used over the last few decades researches and projects to map shallow subsurface structural features of varying interests, the interpretation of the recorded VLF-EM anomalies is mainly carried out using anomaly curves and monograms (Kaikkonen 1979, Saydam 1981). Fraser and Hjelt filtering and subsequent contouring of the observed responses are the most common practices to derive qualitative information about the subsurface (Fraser 1969, Karous and Hjelt 1983).

The VLF-EM theory, technique and details are well described and explained in the literature (Paterson and Ronka, 1971; Philips and Richards, 1975; Wright, 1988; McNeill and Labson, 1991; Hutchinson and Barta, 2002). Mu'awiya et. al. used electrical resistivity method in evaluation groundwater exploration in Adankolo Campus, Lokoja.

Other various workers such as Nurudeen and Amadi, 1990, Olayinka, 1990, Payne, 1988, and Tijani et. al., 2009, utilized electromagnetic profiling/traversing for groundwater exploration in the Nigerian basement complex and delivered successful results.

This study therefore intends to use VLF-EM data to characterize the basement structure of Gofaminth Camp around Ibadan, Southwestern Basement Complex of Nigeria.

Geology of Study Location

The study area, which is a camp falls within Ibadan, Southwestern Nigeria. It is located between longitudes $03^0 55' 49"$E and $03^0 56' 04"$E latitudes $07^0 29' 28"$N and $07^0 729' 58"$N.

The study site generally slopes gently towards the north with few outcrops of migmatitic- gneisses striking NE – SW (Plate 1). The area is predominantly underlain mainly by migmatite gneiss and it is concealed in most part of the site (fig. 1) but only outcrops towards the northern part of the site. It trends at an angle ranging from 002^0 to 012^0 and dips at an angle ranging from 34^0 to 58^0W. The rock is medium to coarse grain with alternations of ill-defined bands of leucosome and melanosome (Plates 2). The other rock types are few outcrops of schist belt and few quartzite. It is also characterized by few joints and fractures with minor intrusions such as quartzo-feldspathic vein of various dimensions. Analysis of the attitudes of the geological structures such as angles of orientation of joints and fractures indicates major structural orientation which trends in northeast – southwest direction (fig. 2). The surface occurrence of these joints and fractures give an idea on the possible direction of groundwater flow. Other rock types include Schist unit and quartzite (fig. 1). They outcrop outside the site within the vicinity of the study area.

Plate 1: outcrop of migmatitic gneiss from the study area

ISSN No. 2454-6194 | DOI: 10.51584/IJRIAS | Volume VIII Issue VI June 2023

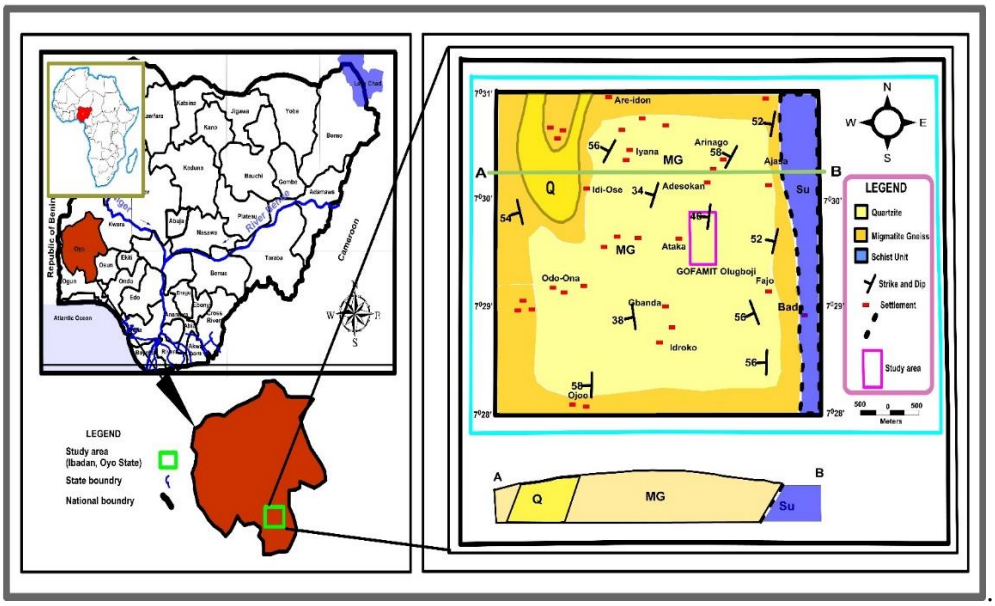

Fig. 1: Geological Map and Geologic Section of the Study Area and Environs.

Plate 2: Outcrop of Migmatitic Gneiss showing alternation of bands

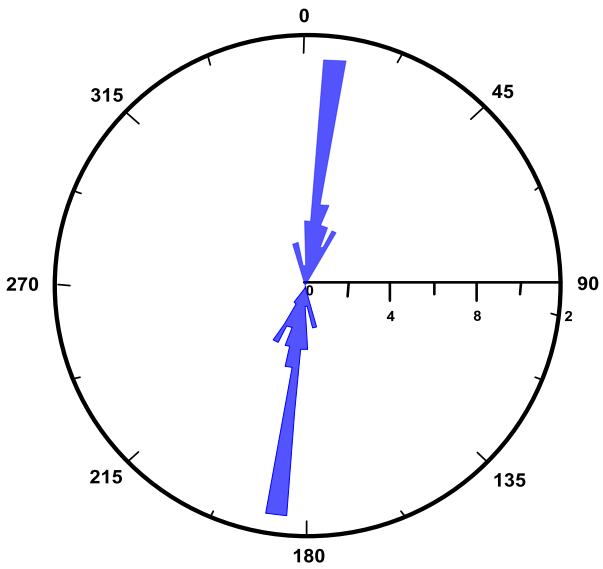

Fig. 2: Rossette Diagram showing trend of Foliation in Migmatitic-Gneisses.

ISSN No. 2454-6194 | DOI: 10.51584/IJRIAS | Volume VIII Issue VI June 2023

II. Materials and Methods

General Background

Basement rock are generally characterized with fractures of various dimension and orientation varying from joint sets, joint system and even master joints depending on their orientation, sizes and concentration. Also some of these joints may be healed by minerals while some might even be barren. Rock outcrops and its associated structures such as foliation, joints, fractures etc. were mapped. Their attributes or attitudes such as strikes and dips were recorded. These basements can easily be isolated by low frequency electromagnetics since it can detect subsurface conductive anomalous zones. Also it does not require contact since it makes use of magnetizing force which induces EM current into the ground.

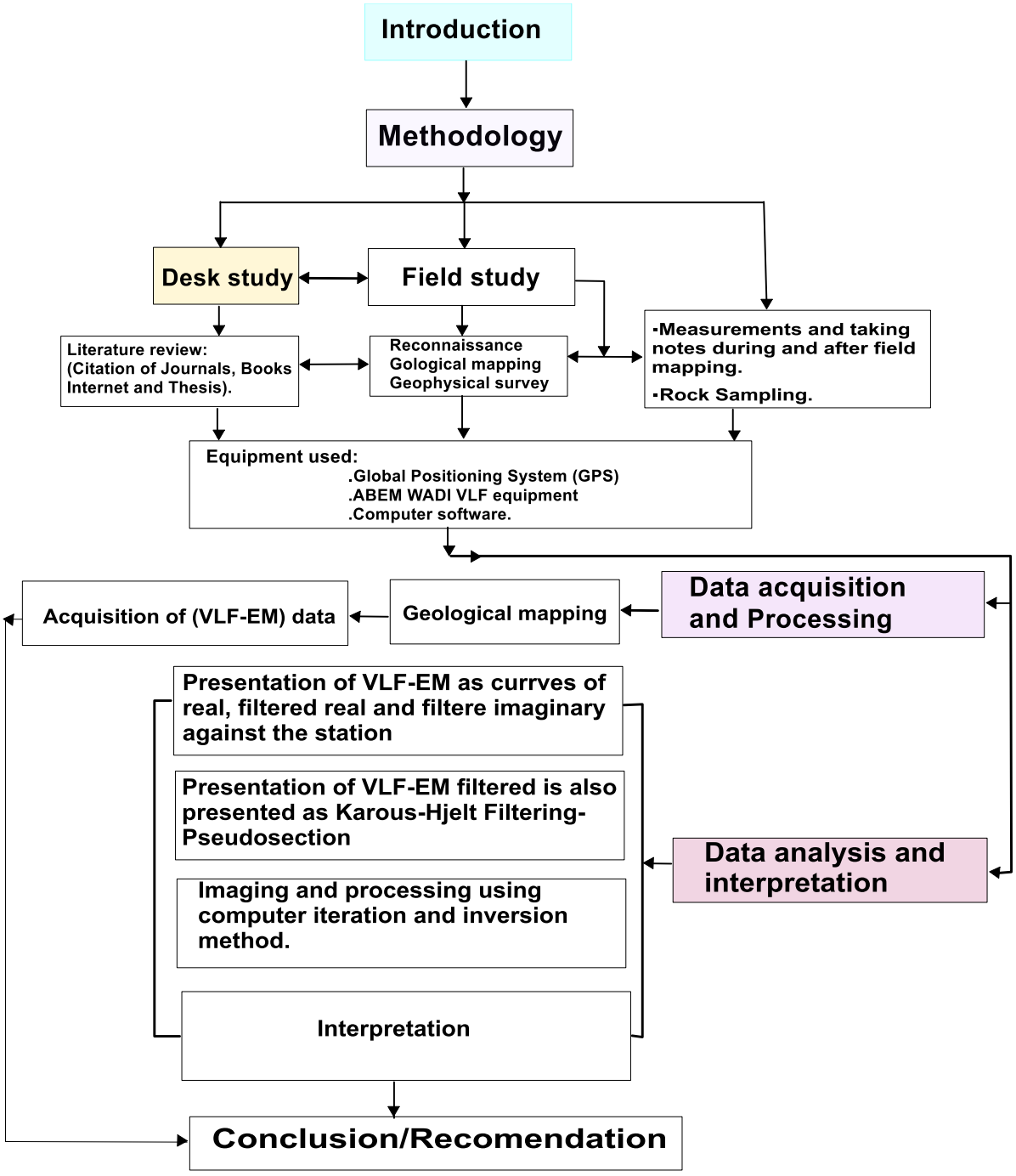

Fig 3: Workflow chart adopted for this research

ISSN No. 2454-6194 | DOI: 10.51584/IJRIAS | Volume VIII Issue VI June 2023

The methodology is summarized in two stages:

- Data acquisition and processing which include geological mapping to determine types of rock in the study location and acquisition of Very Low Frequency electromagnetic (VLF-EM) data
- Data analysis and interpretation which include the presentation of VLF-EM data as curves of raw real, filtered real and filtered imaginary against the stations and again the presentation of VLF-EM filtered real as Karous-Hjelt Filtering Pseudosection.

Interpretation and inferences were drawn from all these above information.

Field Procedure

A total of fifteen (15) VLF traverses were taken in the study area. The antenna unit was kept vertical to avoid error and convenient frequency of 15.1 KHz was used which was selected automatically by WADI through the process of scanning. A constant or fixed traverse direction was maintained.

13 out of 15 profiles were in an East – West direction while the remaining 2 was in a North – South direction with station interval of 10 meter (Fig 4). Those of East – West direction is perpendicular to the geological strike of the structural elements while those of North – South orientation were parallel to the orientation of the geological features.

After the data acquisition, both raw and filtered data of the real and imaginary component of the secondary field were downloaded.

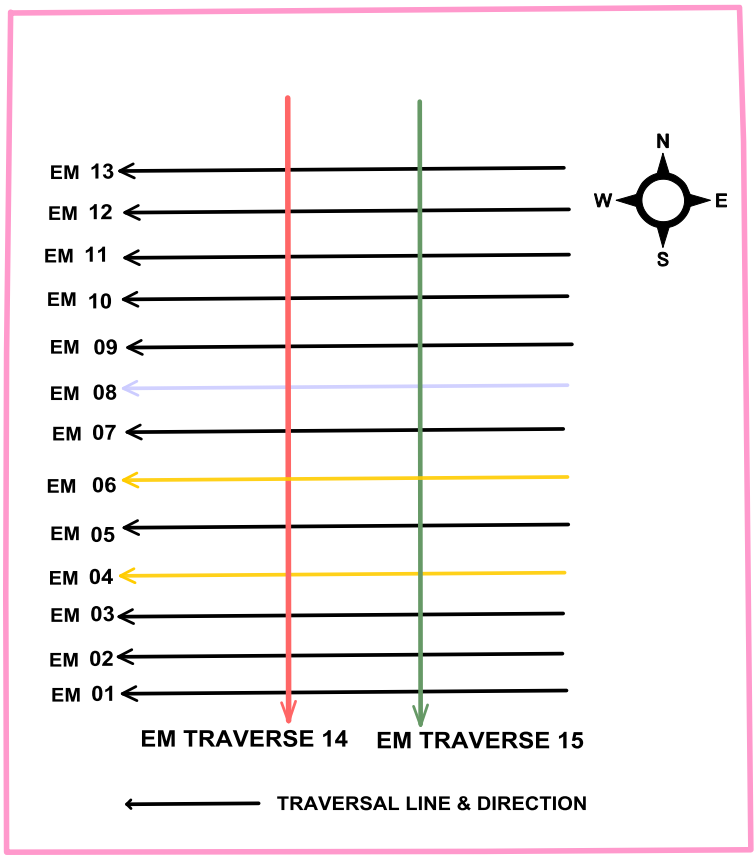

Fig. 4: Profile Outline Showing VLF-EM Traverse.

Principle of Electromagnetic (EM) Method

The VLF method can be effectively used to locate steeply dipping structures which differ from their surroundings hosts in terms of electrical resistance and hence very suitable for the study of basement fracture. The VLF method is a frequency domain electromagnetic method that is propagated by inducing primary EM currents that flow within the periphery of a conductor to generate an eddy current, which in turn generates a secondary EM current. If subsurface material is not a conductor, there will be little or no difference between the transmitted primary EM current and received secondary EM current. But if it is a conductor, the

ISSN No. 2454-6194 | DOI: 10.51584/IJRIAS | Volume VIII Issue VI June 2023

transmitted primary EM current will differ from the received secondary EM current and the amount of difference depends on the conductivity of the subsurface material. This aid in revealing the objects located far beneath the surface and also estimate the electrical conductivity of the buried subsurface materials. EM techniques can be broadly divided into two groups: Frequency Domain and Time Domain but the discussion of the theory will be limited to the frequency domain in this work.

Very Low Frequency EM (VLF- EM) – Is an inductive technique which relies on Very Low Frequency horizontal EM signals from remote military transmitters as an electrical source. Localized conductors, such as water-filled fractures or mineral infillings, cause angular disturbances in this signal which are measured with the VLF-EM instrument.

Very Low Frequency Electromagnetic (VLF) Surveying

Geophysical investigation of the study area is carried out with VLF-EM) method. This was carried out with the aid of WADI instrument strapped on the WADI man. Measurements are carried out along predetermined measurement lines. The WADI utilizes the magnetic components of the electromagnetic field generated by military radio transmitters that use the VLF frequency band. They are used mostly for long-distance communication.

Electrically conductive structures on the surface or underground, even when covered with thick overburden, affect locally the direction and strength of the field generated by the transmitted radio signal. A weak secondary field builds up around the geological structure. This field can be measured and analysed. The WADI measures the field strength and phase displacement around a fracture zone in the rock. In order for induction to occur, the structure must be aligned (roughly) towards the transmitter.

Theory of Electromagnetic Field

All arguments in electromagnetism begin with Maxwell's equations. In particular, he proposed the theory of electromagnetic field, which classifies light as an electromagnetic phenomenon in the same sense as electricity and magnetism. This ultimately led to the recognition of wave nature of matter. The coupling of the electric and magnetic fields is called electromagnetism.

There are four basic equations guiding the propagation and attenuation of electromagnetic waves. These can be derived using the Maxwell's equations, which relates the electric and magnetic field vectors.

The Maxwell's equations are:

1. $\vec{\nabla}.\vec{E} = \frac{\rho}{\varepsilon_\circ}$ (i)

2. $\vec{\nabla}.\vec{B} = 0$ (ii)

3. $\vec{\nabla} \times \vec{E} + \frac{\vec{\delta}B}{\delta t} = 0$ (iii)

4. $\vec{\nabla} \times \vec{B} = \mu_\circ j + \frac{1}{C^2}\frac{\delta E}{\delta t}$ (iv)

Note that from equation (i)

$\vec{\nabla}.\vec{E}\ \varepsilon_\circ = \vec{\nabla}.\vec{D} = \rho$ where $\vec{E}\ \varepsilon_\circ = D$

From equation (ii)

$\vec{\nabla}.\vec{H} = 0$

$\mu_\circ \vec{H} = \vec{B}$

From equation (iii)

$\vec{\nabla} \times \vec{E} = -\frac{\vec{\delta}B}{\delta t}$

From equation (iv)

$\vec{\nabla} \times \vec{B} = \mu_\circ j + \frac{1}{C^2}\frac{\vec{\delta}E}{\delta t}$

$\vec{\nabla} \times \vec{H} = j + \frac{1}{\mu_\circ C^2}\frac{\vec{\delta}E}{\delta t}$

$\vec{\nabla} \times \vec{H} = \sigma\varepsilon_\circ + \varepsilon_\circ \frac{\vec{\delta}E}{\delta t}$

ISSN No. 2454-6194 | DOI: 10.51584/IJRIAS | Volume VIII Issue VI June 2023

Where

$j = \sigma \varepsilon_\circ$

$\frac{1}{c^2} = \mu_\circ \varepsilon_\circ$

$\vec{E}$ – Electric field intensity (V/ m^2), $\vec{D}$ – Electric displacement (V/ m^2), $\vec{H}$ – Magnetic field intensity (testa), $\vec{B}$ – Magnetic flux density, $\varepsilon_\circ$ – Permittivity of a medium,

$\mu_\circ$ – Permeability of free space ($4\pi \times 10^{-7}$ Henry/m), j– Current density

σ – Conductivity (mho/m) simens, C – Speed of light, ρ – Electric charge density

There are four fundamental equations of electromagnetism that apply to all electromagnetic phenomena in media that are at rest with respect to the coordinate system in use. They are valid for non-homogeneous, non-isotropic media. The two electromagnetic wave equations for the propagation of magnetic and electric fields can be deduced from the above equations. Taking the curl of equation (iii) will give the electromagnetic wave equation for propagation of field vectors.

5. $\nabla^2 \vec{E} = \varepsilon_\circ \mu_\circ \frac{\overrightarrow{\delta^2 E}}{\delta t^2} + \mu_\circ \sigma \frac{\vec{\delta} E}{\delta t}$ (v)

6. $\nabla^2 \vec{E} - \varepsilon_\circ \mu_\circ \frac{\overrightarrow{\delta^2 E}}{\delta t^2} - \mu_\circ \sigma \frac{\delta E}{\delta t} = 0$ (vi)

The EM wave equation for propagation of magnetic field vectors can be deduced by taking the curl of equation (iv)

7. $\nabla^2 \vec{H} = \varepsilon_\circ \mu_\circ \frac{\overrightarrow{\delta^2 H}}{\delta t^2} + \mu_\circ \sigma \frac{\vec{\delta} H}{\delta t}$ (vii)

8. $\nabla^2 \vec{H} - \varepsilon_\circ \mu_\circ \frac{\overrightarrow{\delta^2 H}}{\delta t^2} - \mu_\circ \sigma \frac{\delta H}{\delta t} = 0$ (viii)

Equations (vii) and (viii) obtained above govern the electromagnetic field in a homogeneous, linear medium in which the change density is zero, whether the medium is conductive or non-conductive.

Considering the angular frequency of low electromagnetic fields,

9. $\omega = 2\pi f$ (ix)

10. $\varepsilon(t) = \varepsilon_\circ e^{jwt}$ (x)

11. $H(t) = H_\circ e^{jwt}$ (xi)

If it were in time variation, that is sinusoidal, substituting equation (vii), (viii), (ix) into equation (v) and (vii), we have,

12. $\nabla^2 \vec{E} = \varepsilon_\circ \mu_\circ jw^2 \vec{E} + \sigma \mu_\circ jw^2 \vec{E}$ (xii)

13. $\nabla^2 \vec{H} = \varepsilon_\circ \mu_\circ jw^2 \vec{H} + \sigma \mu_\circ jw^2 \vec{H}$ (xiii)

These equations (xii) and (xiii) are the electromagnetic equation for propagation of electric and magnetic field vectors in an isotropic, homogeneous medium having conductivity σ, permeability $\mu_\circ$, and permittivity $\varepsilon_\circ$.

The Depth of Penetration by Electromagnetic Field

General electromagnetic survey method has shallow depth of penetration. The depth of penetration also known as the skin depth "*d*" is the attenuation distance in conductors.

Hence, "*d*" = $\left(\frac{2}{\omega \sigma \mu}\right)^{\frac{1}{2}}$

The term measures the depth at which the electric field falls to $\frac{1}{e}$ of its value at the surface. The skin depth decreases as the conductivity σ, permeability $\mu_\circ$, and frequency

f, (i.e. $2\pi f = \omega$) increase.

A very simple diagram that shows field induction caused by a fracture zone is presented in fig. 5.

ISSN No. 2454-6194 | DOI: 10.51584/IJRIAS | Volume VIII Issue VI June 2023

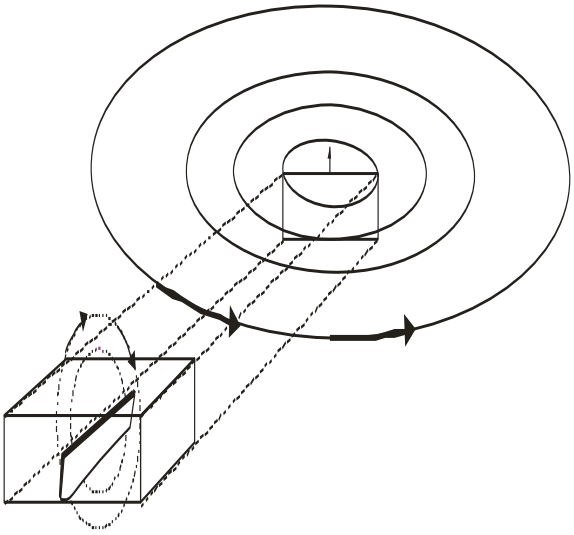

Fig. 5: A schematic diagram of VLF propagating principle

ABEM WADI Instrument

This a receiver unit of the VLF system which records both the primary field from the transmitter that travels via the surface and the secondary field generated from the subsurface conductor. The primary field that propagates through the ground induces a current flow in the periphery of the conductor. This eddy current in turns generate a secondary EM field which is recorded by the receiver (WADI instrument). The WADI instrument is portable and mounted on a belt worn by the user.

Below is the table (Table 1) of frequently encountered geological materials with their resistivity values.

Table 1: Typical resistivity (r) and depth of penetration (d) values for frequently encountered geological materials.

MATERIALS	RESISTIVITY r (Ωm ohm-m)	DEPTH d (m)
Hard rock (granite)	> 5000	> 300
Clay	10-100	15-40
Dry sand	200-500	50-300
Wet sand	50-200	30-60
Fresh water	50-200	30-60
Saline water	1-10	4 -15

One measure of the extent to which the field is affected is called depth of penetration. This is often designated by means of the Greek letter ∂ (delta).

$\partial = 503\sqrt{(\rho/f)}$ Where r is resistivity in Ωm, and f is frequency in Hz.

Therefore, the depth of penetration is determined by the resistivity (inverse of conductivity) of the overlying material and the target.

Anomaly

VLF method can be used to reveal elongated, steeply dipping structures with large cross-sections and low resistivity. A deviation from a normal WADI reading is called an anomaly indication (fig. 6). In Electromagnetic prospecting, in addition to amplitude, phase displacement relative to the primary field is also taken into consideration. For VLF however, instead of using the term amplitude and phase, real and imaginary components respectively which are both measured by WADI instrument are used. But most of the useful information is found in the real part. The real component is the part of the resulting secondary field which are in phase with the primary field from the transmitter while the imaginary (quadrature) component is the resulting secondary field which are 90^0 out of phase with the primary field. The anomaly indication shown in Fig. 5 is linked to the real part.

ISSN No. 2454-6194 | DOI: 10.51584/IJRIAS | Volume VIII Issue VI June 2023

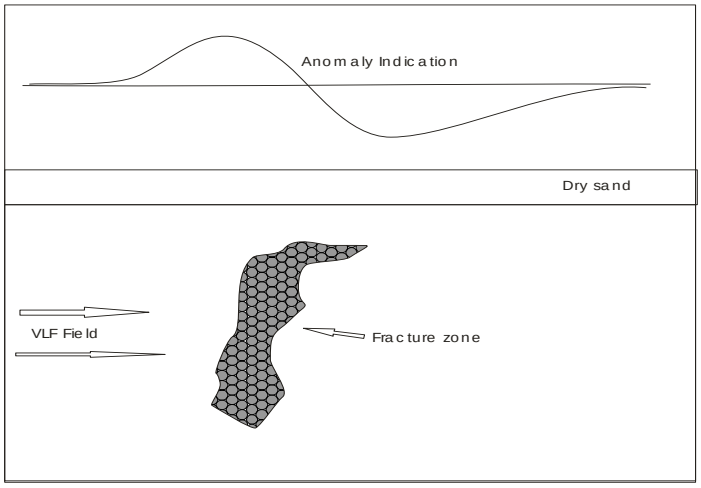

Fig. 6: A typical anomaly indication (original raw data).

In a simple case shown in Fig. 6, a positive bulge (peak) appears to the left of the subsurface structures and a negative bulge appears to the right of it. It is easy to locate the fracture zone. The structure is at the position of cross-over point (the point where the dip angle change sign from positive to negative through zero). But for complicated cases that involve a number of subsurface bodies, it is very difficult to ascertain the positions of individual bodies, and hence the need for data filtering.

Filtering

Processing the measured VLF data using numeric algorithm can make it easier to interpret results. Here, an important step forward was taken in 1963 when a description of a filtering method was published in "Linear Filtering of Dip-Angle Measurements" by M. Karous and S.E Hjelt. This method vastly facilitates the interpretation of anomaly indications.

Filter action can be expressed mathematical in terms of convolution.

$F_0 = -0.102*H_{-3} + 0.059*H_{-2} – 0.561*H_{-1} + 0*H_0 + 0.561*H_1 – 0.059*H_2 + 0.102*H_3$

Where H_{-3} through H_3 are the original VLF data (as shown in Fig.5 for example), and F_0 is the filtered result.

The filtered coefficients are moved along the profile station by station and in this type of filtering, the distance between stations H_0, H_1, H_2 … can be selected or desired. Information about a specific depth can be obtained by selecting an appropriate between- station distances.

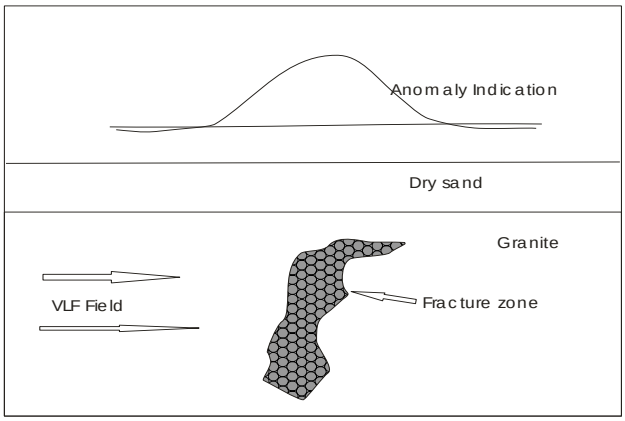

Fig. 7: A typical anomaly indication (Filtered data)

The filtered curve (fig.7) can be considered a representation of secondary currents in the ground. Filtering comprises a numeric algorithm-a black box that can be used to convert complicated VLF anomalies to curves that are easier to interpret. A comparison between the original data (fig. 6) and the filtered data (fig.7) shows that after filtering it is much easier to locate a fracture zone since all that is needed is to look for the highest point on the curve. The peak of the bulge now appears directly over the fracture zone.

ISSN No. 2454-6194 | DOI: 10.51584/IJRIAS | Volume VIII Issue VI June 2023

III. Model for Data Interpretation

Interpretation is mostly based on the real part of the anomaly indications. Useful information can also be obtained from the comparison or ratio of real to imaginary part. This gives information about the electrical properties and geometry of the conductor.

It is important to carry out measurement along profiles that are sufficiently long, since this gives complete anomaly indication as in figure 8(a).

The curve fluctuates around zero initially and rises to form a high positive bulge (peak), after which it drops to zero again.

Fig. 8(b) shows the difference between the anomaly indications obtained from a deep structures and one that is close to the surface. They differ mostly with regard to the widths and amplitudes of the anomaly indications. Deeper anomaly readings are wider, but have lower amplitudes. However, a low amplitude can also result from a poor conductor (a geological structure that has medium to low electrical conductivity).

As earlier mentioned, the imaginary part can also reveal important information regarding the property of the conductor. Fig. 8(c) reveals a typical anomaly indication obtained for an ore body or fracture zone that contains saltwater (for example).

This out-of-phase component can also indicate a positive anomaly, depending on extent and resistivity of the overburden.

Also, in fig. 8(d) a typical anomaly indication obtained for structure having relatively high resistivity (poor conductor), a fracture zone containing fresh water for example, can be seen.

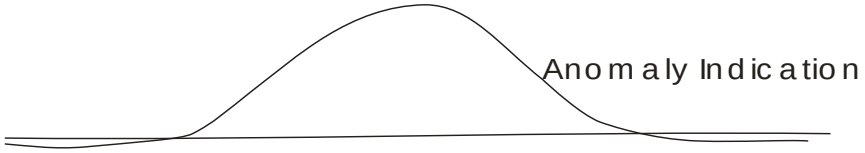

(a). complete anomaly indication

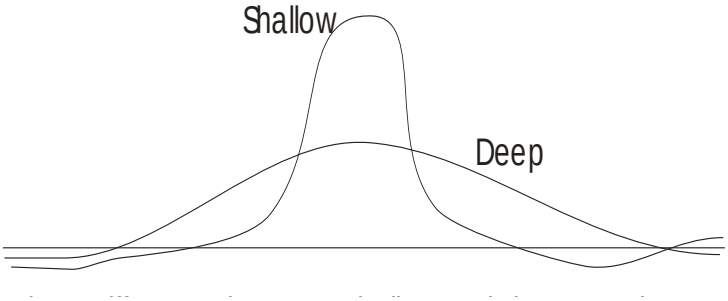

(b). Difference between shallow and deep conductor

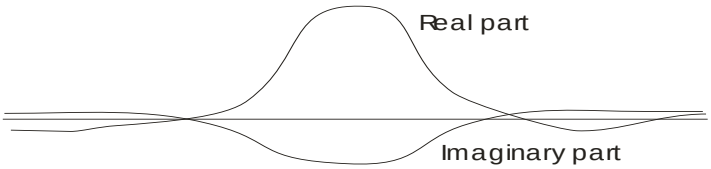

(c). Typical anomaly from a good conductor

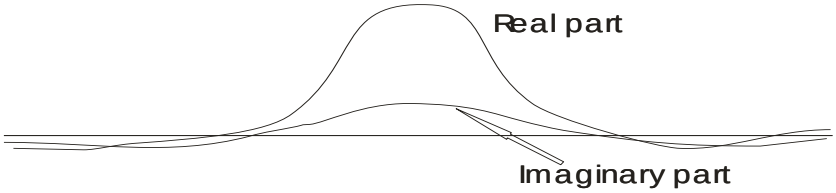

(d). Typical anomaly from a poor conductor

Fig. 8: Anomaly indications for (a) a long profile line (b) Shallow and Deep conductors (c) a good conductor (d) a poor conductor. (ABEM WADI Interpretation Guide)

ISSN No. 2454-6194 | DOI: 10.51584/IJRIAS | Volume VIII Issue VI June 2023

Double Closely Spaced-Fracture

It is usually difficult to identify closely spaced fracture from the original raw data but the filtered data revealed it clearly (Fig. 9) and this reveals two fracture zones located 40 meters apart.

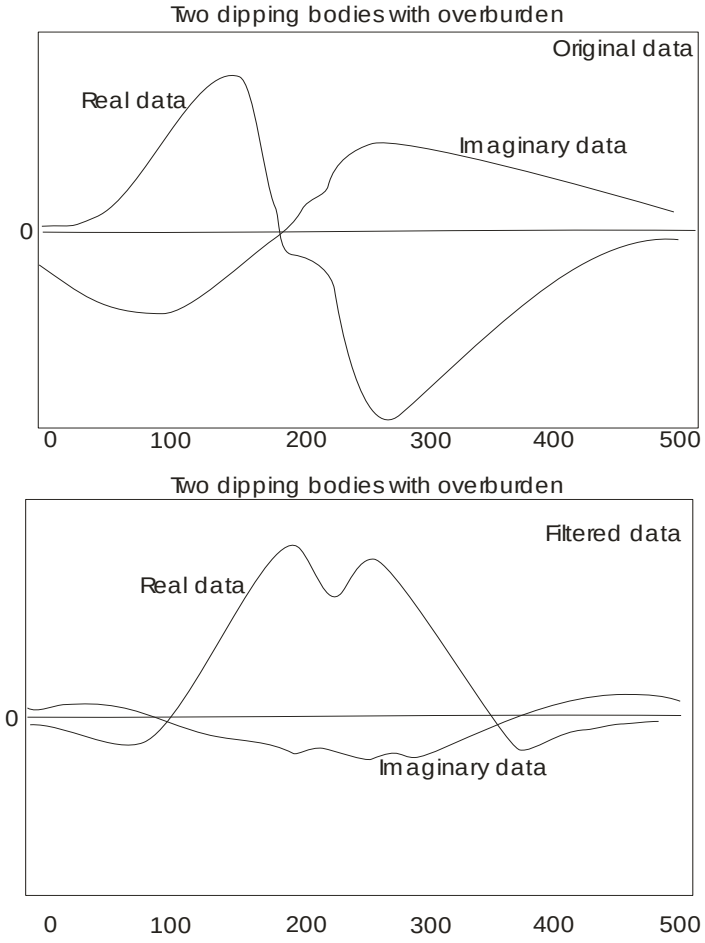

Fig. 9: Anomaly indication from a double zone or fracture (ABEM WADI Interpretation Guide)

IV. Results, Analysis and Discussions

Geological Investigation

The study area is underlain by magmatitic-gneisses which are hard basement rock with fractures and veins and some minor faults. The rock outcrop is also characterized by structural elements such as joints, quartz and quartzo-feldspathic veins, banding and gneissic layering.

Geophysical Investigation

The only use of the filtered imaginary is when it is plotted alongside with filtered real on the same scale in order to provide information about the electrical property of the conductor (steeply dipping fracture). Apart from that, the crossovers of in-phase (real component) and out-of-phase (imaginary or quadrature components) are inferred to be the conductor or basement fracture axes and orientation (Wright, 1988), and this case are caused by the accumulation of water and or other mineralized material within the fracture. Furthermore, the asymmetry in the in-phase and out-of-phase components is caused by the dipping nature of conductors, wherein the larger anomaly peak identifies the down-dip side (Coney, 1977; Baker and Myers, 1979). Therefore, the VLF-EM in-phase and out-of-phase components are presented in the form of stacked profiles in Fig. 10(a&b), 12(a&b), and 14(a&b). The profiles (Fig. 10b, 12b, and 14b) indicate that the fractures are striking almost in N-S, NE-SW and NW-SE direction which is generally the direction of basement fracture imposed by the Pan African orogenic//tectonic episodes and this correlate well with the rose diagram of figure 2 derived from the surface mapping of fractures exposed on the surface from the area. It also indicates that they generally dip vertically.

ISSN No. 2454-6194 | DOI: 10.51584/IJRIAS | Volume VIII Issue VI June 2023

The filtered real is presented as Fraser filtering curves or profiles and Karous – Hjelt (K-H) pseudo-section and Karous-Hjelt filtering and because of space about three of these are presented as fig. 11, 13 and 15 as a representative samples of others for discussion. The interpretation was based on these profiles and K – H pseudo-sections and Karous-Hjelt filtering and they were basically qualitative or semi quantitative (Karous and Hjelt 1983). The positive peaks mapped as fractures on the filtered real. They are zones of interest in groundwater extraction in basement complex terrain. The conductivity is colour coded increasing from left to right. According to McNeil and Labson, 1992, the high conductivity zones with red signatures may have resulted from the accumulation of water in the fracture or build-up of clayey materials.

GOFAMINT EM Traverse 03: It has a **p**rofile length of 180 meters and it is oriented in E-W direction. It shows one prominent conductive anomalous zone at a surface distance of 55 meters (Fig: 11) which shows that the causative body is a good conductor (fracture) likely to contain fresh water and/or polarizable conductive-rich mineral as shown in K-H pseudo-sections (fig. 11). An existing borehole contains usable quantity of water and therefore serves as control. The fracture extends from depth of approximately 10m to 30m and even beyond and it has slightly conductive units (depicted by yellow colouration) surrounding the very high conductive zone (red colouration) at the centre indicating gradation in conductivity as indicated in the Karous-Hjelt filtering (fig. 11).

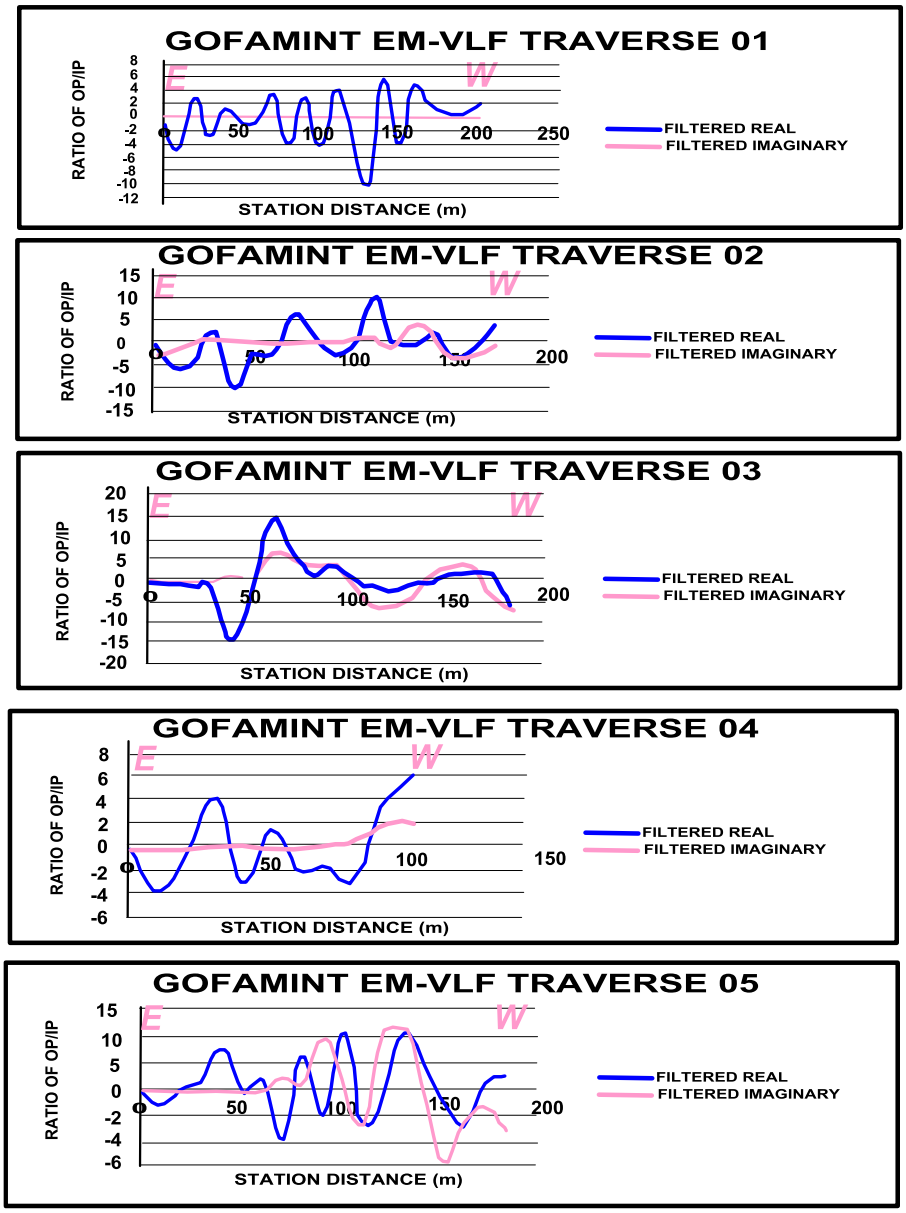

Fig. 10a. Stacked profiles of in-phase and out-of-phase components of the VLF-EM.

ISSN No. 2454-6194 | DOI: 10.51584/IJRIAS | Volume VIII Issue VI June 2023

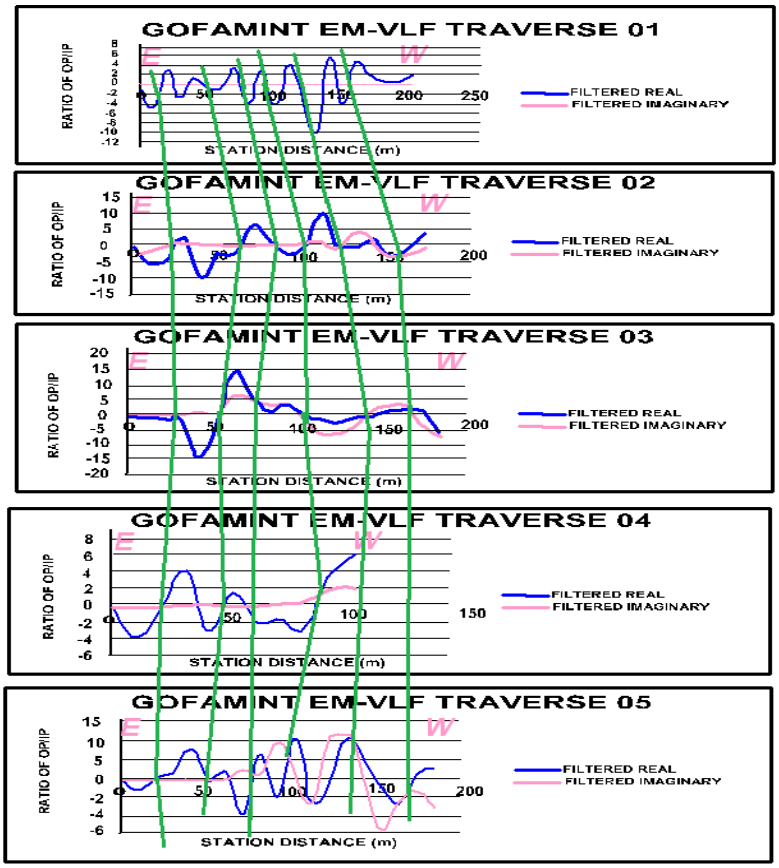

Fig. 10b. Stacked profiles of in-phase and out-of-phase components of the VLF-EM showing basement fracture axis (Green).

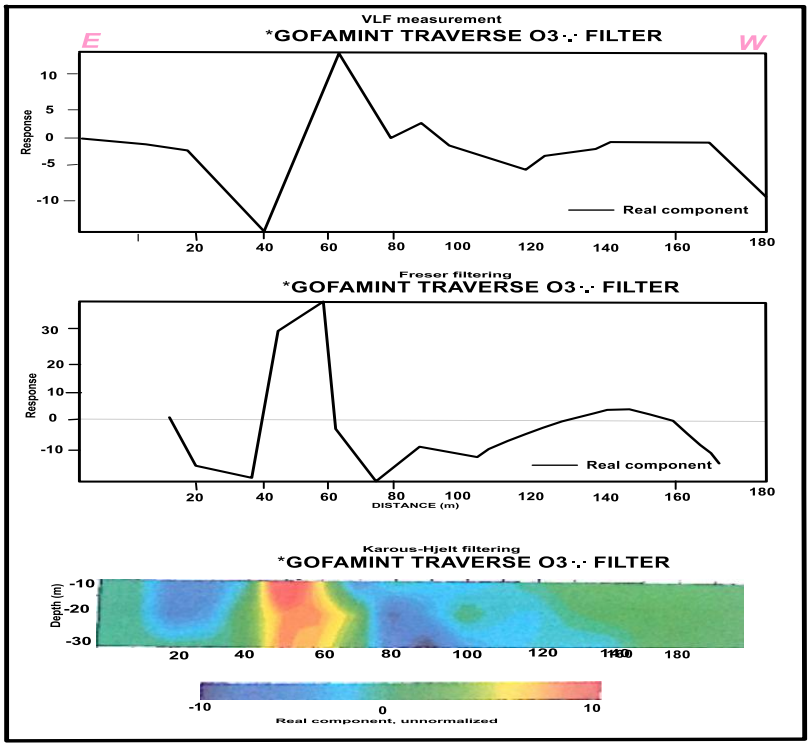

Fig. 11: Plot of Filtered Real, Fraser filtered Real and Karous-Hjelt Filtering.

ISSN No. 2454-6194 | DOI: 10.51584/IJRIAS | Volume VIII Issue VI June 2023

GOFAMINT EM Traverse 08: The profile has a length of 290 meters and also in an E-W direction, there are series of high and low positive peaks (Fig 13) the anomalies at the two extreme ends seems to result from fractures containing freshwater. The first anomaly is centred at a surface distance of 50m and occur at depth between 20-35m while the second anomaly is a double fracture which joins together at depth and they occur at a surface distance of 240m and depth between 10-35m beneath the surface (Fig. 13). Borehole can be suggested at this second position of conductivity anomaly.

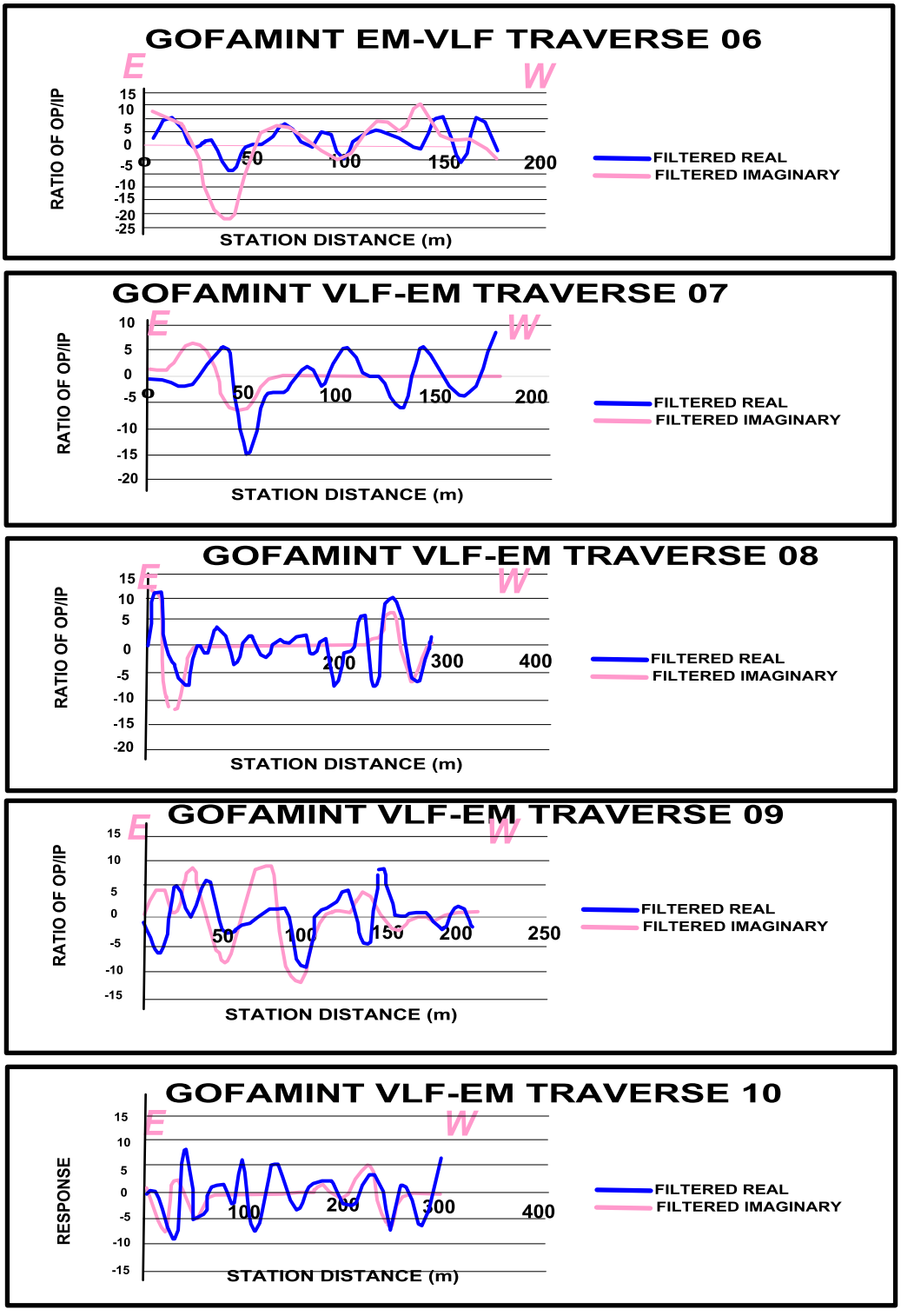

Fig. 12a. Stacked profiles of in-phase and out-of-phase components of the VLF-EM.

ISSN No. 2454-6194 | DOI: 10.51584/IJRIAS | Volume VIII Issue VI June 2023

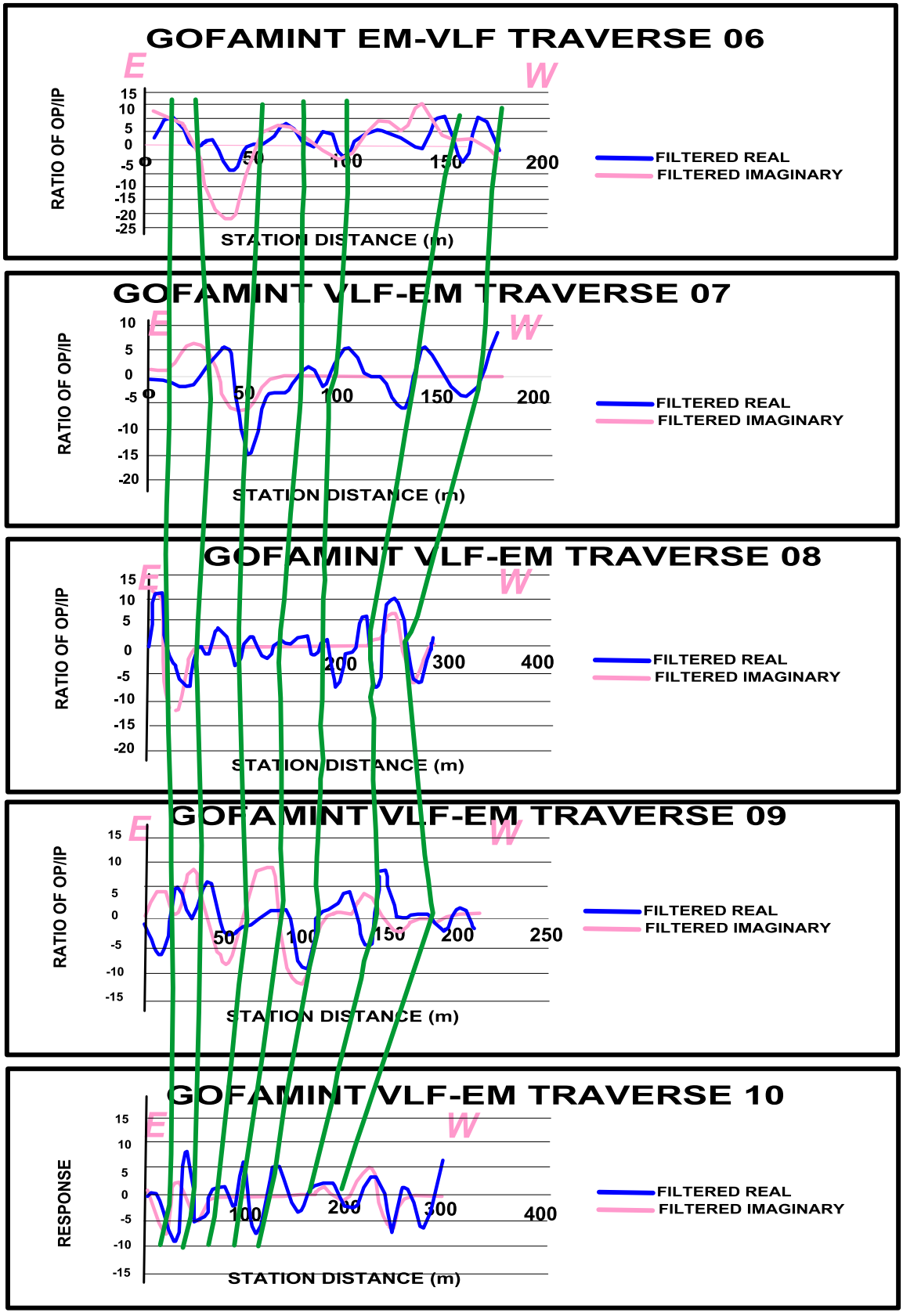

Fig. 12b. Stacked profiles of in-phase and out-of-phase components of the VLF-EM showing basement fracture axis (Green).

ISSN No. 2454-6194 | DOI: 10.51584/IJRIAS | Volume VIII Issue VI June 2023

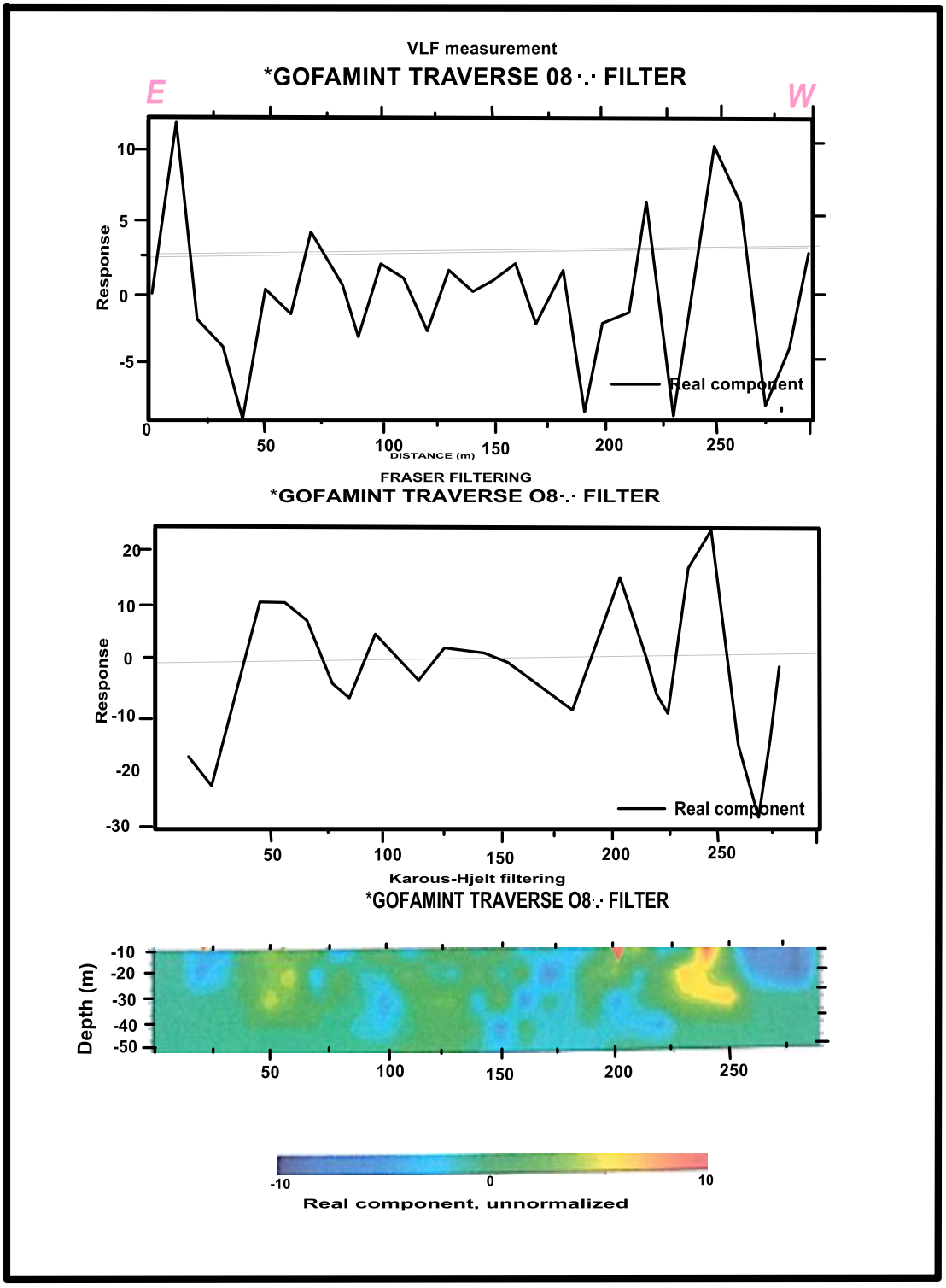

Fig. 13: Plot of Filtered Real, Fraser filtered Real and Karous-Hjelt Filtering.

GOFAMINT EM Traverse 11: This has a traverse length of 280 meters with measurement taken in an E-W direction. One prominent anomaly peak was observed at station point 200-230 meters which are double fractures closely-spaced and joined together at depth. They occur within the depth of 10-40m. They all tend to be poor conductors having tendency to contain water (Fig. 15). At other surface locations the anomalies are not pronounced (Fig. 15). They occur as pocket of conductive zones in the Karous-Hjelt (K-H) pseudo-section.

ISSN No. 2454-6194 | DOI: 10.51584/IJRIAS | Volume VIII Issue VI June 2023

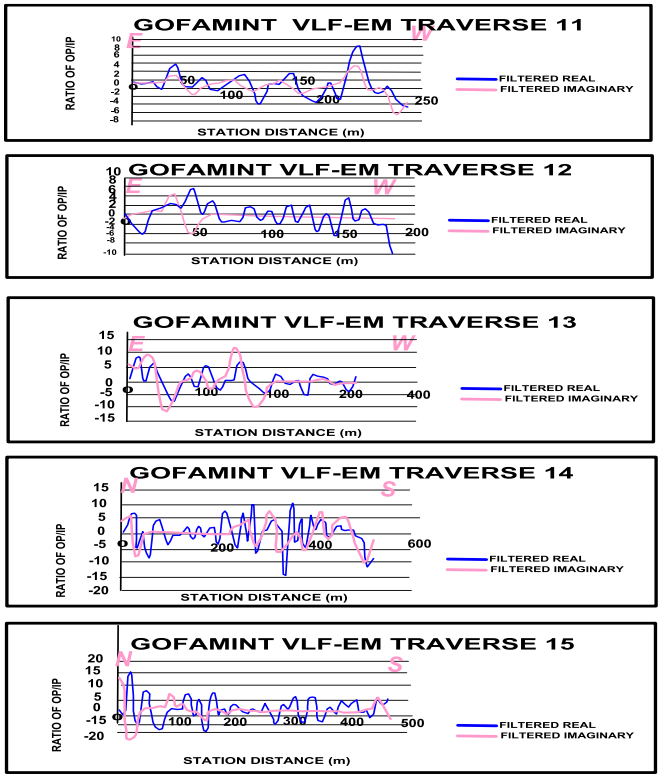

Fig. 14a. Stacked profiles of in-phase and out-of-phase components of the VLF-EM.

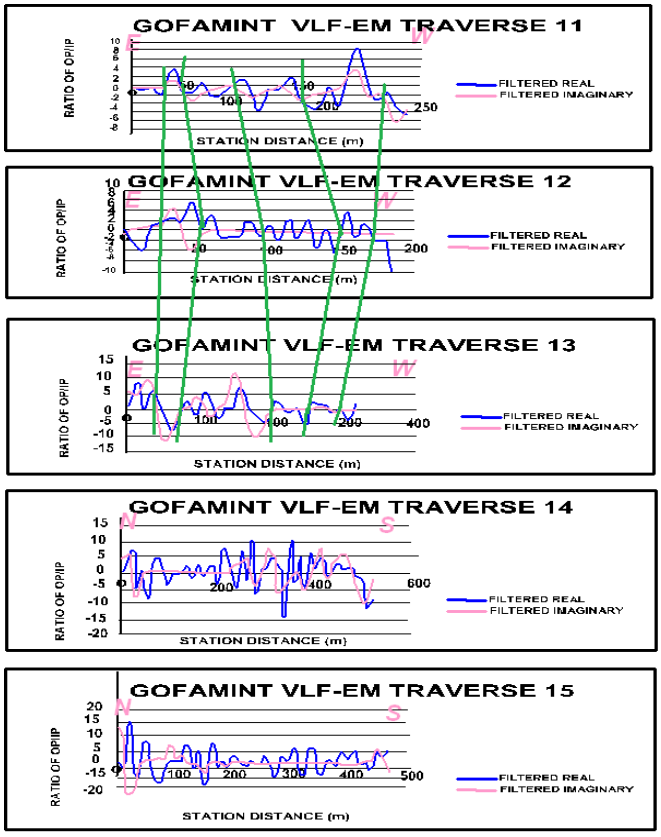

Fig. 14b. Stacked profiles of in-phase and out-of-phase components of the VLF-EM showing basement fracture axis (Green).

ISSN No. 2454-6194 | DOI: 10.51584/IJRIAS | Volume VIII Issue VI June 2023

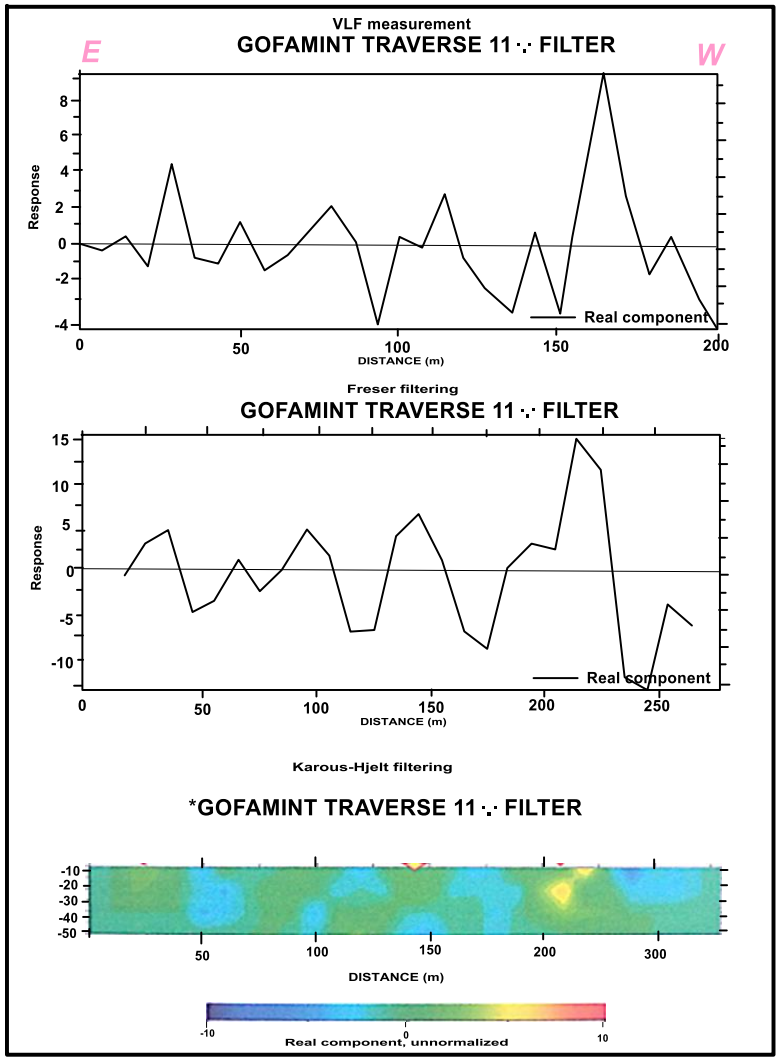

Fig. 15: Plot of Filtered Real, Fraser filtered Real and Karous-Hjelt Filtering.

V. Conclusion

The study area was investigated using geological and geophysical techniques (VLF-EM) to reveal the subsurface geology and characterize and model the basement structure. Geological mapping shows an outcrop of Migmatite-gneiss striking NW-SE and dipping in Western direction which are characterized by structural features such as joints, fractures, minor faults and foliation. Other rock types such as Schist unit and quartzite were also encountered around the environs of the study area. Conductive zones interpreted to be steeply dipping or vertical basement fracture were delineated from VLF-EM data. These direction of the basement fracture striking N-S and NW-SE and NE-SW isolated from this VLF profile coincides with regional trend impose on the basement rock by Pan African orogeny.

The VLF-EM results serve as the basis for the characterization of the basement structural features though they are not all that prominent in some area. Regions with high conductivity (from VLF-EM) are delineated as the basement aquifer and or conductive ore body.

VI. Recommendation

The use of LAND SAT IMAGERY / RADAR SENSING should be used in conjunction with other geophysical methods such as induced polarization (IP), resistivity, seismic refraction, magnetic and gravity. These methods are also capable of detecting fractures, contacts, joints and depressions which tend to harbour groundwater and mineralization within the basement terrain.

Finally, geochemical exploration should be carried out in conjunction with these geophysical investigations to give more details on the mineralization potential of the area.

ISSN No. 2454-6194 | DOI: 10.51584/IJRIAS | Volume VIII Issue VI June 2023

References

1. ABEM WADI Interpretation Guide; Theory, practice and case stories for WADI operators. Issued by ABEM AB, Box 20086, S-161 02 Bromma Sweden. Telex: 13079 ABEM S, Tlelfax: +468 28 11 09.
2. ABEM (2007). A Nitro Consultant company, international frequency list, ABEM printed matter No. 93062: WWW. Abem.se/products/wadi/vlf-freq.pdf. accessed June 18, 2007.
3. Andarawus Y. Nur A. Musa N. Adamu A. Mu'awiya BA, (2022). Geoelectric Investigation for Aquifer Characterization in Boi and Environs, Bauchi State, Northeast, Nigeria. Dutse Journal of Pure and Applied Sciences (DUJOPAS), Vol. 8 No. 2a June 2022
4. Anomohanran, O. (2011a). Determination of Groundwater in Asaba, Nigeria using Surface Geoelectric Sounding. International Journal of Physical Science 6:7651-7656
5. Anomohanran, O. (2011b). Underground Water Exploration of Oleh, Nigeria using the Electrical Resistivity Method. Scientific Research Essays, 6: 4295-4300.
6. Atakpo, E. & M. O. Ofomola, (2012). Hydrologeologic Investigation using Vertical Electrical Sounding Method in Agbarha Otor, Delta State Nigeria. Nigeria Journal of Science Environment 11:95-103.
7. Baker, H. A., & J. O. Myers, (1979). VLF-EM model studies and some simple quantitative applications to field results: Geoexploration, **17**, 55–63.
8. Changde, A. N, Mu'awiya BA, Simon D.C, Ernest O.A, Kizito O.M, Godwin O.A and Okiyi, I.M., (2022). Electric Resistivity for Evaluating Groundwater Potential Along he Drainage Zones In The Part Of Jos North, Plateau State, Nigeria. European Journal of Environment and Earth Sciences Vol 3 | Issue 6 | November 2022 3(6), 59–68. https://doi.org/10.24018/ejgeo.2022.3.6.347
9. Coney, D. P., (1977) Model studies of the VLF-EM method of geophysical prospecting: Geoexploration, **15**, 19–35.
10. Ezeh, C.C. and Ugwu, G. Z. (2010). Geoelectrical Sounding for Estimating Groundwater Potential in Nsukka L.G.A. Enugu State, Nigeria. International Journal o PhysicalScience 5: 415-420.
11. Faruk, M.U (2019). Application of VLF-EM method for base metal exploration in Gwani area (Misau 107), Jigawa state, Nigeria. International Journal of Advanced Geosciences. International Journal of Advanced Geosciences, 7 (2) (2019) 186-193.
12. Fisher, G., B.V. Le Quang, and I. Muller, (1983) VLF ground surveys, a powerful tool for the study of shallow two-dimensional structures: Geophysical Prospecting, **31**, 977–991.
13. Fraser D C (1969) Contouring of VLF-EM data Geophysics 34 958–967.
14. Hayles J G and Sinha A K. (1986) A portable local loop VLF transmitter for geologica fracture mapping: Geophysical prospecting, 34, 873 - 896.
15. Hutchinson, P. J., and L. S. Barta, 2002, VLF surveying to delineate long wallmine induced fractures: The Leading Edge, **21**, 491–493.
16. Iserhien – Emekeme, R. E., E. A. Atakpo, O. L. Emekeme and O. Anomohanran, (2004). Geoelectric Survey for Groundwater in Agbede Etsako West L.G.A., Edo State. Advanced National Applied Science Resource 2: 65-72.
17. Kaikkonen P (1979) Numerical VLF modeling Geophys. Prospect. 27 815–834.
18. Karous M.R. and Hjelt, S.E (1983) Linear Filtering of VLF Dip Angle Measurements Geophysical Prospecting, 31: 782-794.
19. Magawata, U. Z., Yahaya, M. N., Basiru, Q. (2019) Delineation of Fracture Zones for Groundwater Exploration Using Very Low Frequency Electromagnetic (VLF-EM) Method in A Sedimentary Complex TERRAIN: a Case Study of Kebbi State University of Science and Technology Aliero, Northwestern Nigeria. IOSR Journal of Applied Geology and Geophysics (IOSR-JAGG) e-ISSN: 2321–0990, p-ISSN: 2321–0982.Volume 7, Issue 5 Ser. I, PP 59-69
20. McNeil J.D., Labson V.F., (1991). Geological mapping using VLF radio fields. InNabighian, M.C. (Ed.), Geotechnical and Environmental Geophysics Review and Tutorial, vol 1. Society of Exploration, Tulsa, pp. 191-218.
21. Molua, O.C. and J.U. Emagbetere. 2005. Delineation of Water Table using Electrical Sounding Technique: A Case Study of Afuze, Edo State, Nigeria. Journal of Nigeria Association of Mathematics and Physics 5:457-464.
22. Mu'awiya. B.A, Nanfa, C. A., Hassan, J. I., Yahuza, I., Christopher, S. D., & Aigbadon, G.O. (2022). Application of Electrical Resistivity for Evaluation of Groundwater Occurrence Within Adankolo Campus and Environs, Lokoja North Central, Nigeria. European Journal of Environment and Earth Sciences, 3(1), 14–22. https://doi.org/10.24018/ejgeo.2022.3.1.235
23. Nurudeen, S.I, and Amadi, UMP, (1990). Electromagnetic survey and search for Groundwater in the Basement Complex of Nigeria. Journal of Mning and Geology 26 (1), 45-54.
24. Ogilvy R D and Lee A C (1991) Interpretation of VLF-EM in-phase data using current density pseudosections Geophys. Prospect. 39 567–580.

ISSN No. 2454-6194 | DOI: 10.51584/IJRIAS | Volume VIII Issue VI June 2023

25. Olayinka, A.I 1990. EM Profiling for groundwater in Precambrian basement complex area of Nigeria. Nordic Hydrology 21, 67-76.
26. Parker M E (1980) VLF electromagnetic mapping for straband mineralization near Aberfeldy Scondland Trans. Inst. Mining Metall. B 89 B123–133.
27. Paterson, N. R., and V. Ronka, 1971, Five years of surveying with the very low frequency electromagnetic method: Geoexploration, **9**, 7–26.
28. Payne, M.I (1988). Electromagnetic Traversing method of Groundwater exploration in Crystalline Rock Terrain. Journal of Mining and Geology 15(2) 863-874.
29. Phillips W J and Richards W E 1975 A study of the effectiveness of the VLF method for the location of narrow mineralized zones Geoexploration 13 215–226.
30. Ramesh Babu V, Ram S and Sundararajan N 2007 Modeling of magnetic and VLF-EM with an application to basement fractures: a case study from Raigarh, India Geophysics 71 133–140.
31. Saydam A S 1981 Very low frequency electromagnetic interpretation using tilt angle and ellipticity measurements Geophysics 46 1594–1606.
32. Sundararajan N, Chary M N, Nandakumar G and Srinivas Y 2007 VLF and VES—an application to groundwater exploration, Khammam, India The Leading Edge 26 708–716.
33. Wright J L 1988 VLF Interpretation Manual (Concord, Ontario: EDA Instruments, now Scintrex, Ltd).